Adv Syst Sci Appl 2023; **01**; 99-114
Published online at https://ijassa.ipu.ru.

Numerical Investigation of Fluid-Structure, Thermal Coupling for a Heated Slab

Oudrane A.[1*], Aour B.[2], Hamouda M.[1], Chesneau X.[3], Zeghmati B.[3], Balti J.[4]

[1)] *Laboratory of Sustainable Development and Informatics (LDDI), Faculty of Science and Technology, Ahmed Draya University of Adrar, Algeria*

[2)] *Laboratory of Applied Biomechanics And Biomaterials (LABAB), BP 1523 El Mnaouer, National Polytechnic School of Oran-Maurice Audin (ENPO-MA), 31000, Oran, Algeria*

[3)] *Laboratory of Mathematics and PhySics Groups of Energy Mechanics (LAMPS), university of Perpignan Via Domitia, 52, Avenue Paul Alduy, 66860 Perpignan cedex France*

[4)] *Department of Physics, Faculty of Science, University of Carthage, 7021 Jarzouna, Tunisia*

Abstract: This work focuses on a numerical analysis of fluid-structure thermal coupling in a heating slab. The latter consists of a rectangular cross-section duct located in the concrete slab of a discredited habitat. We modeled the thermal transfers of fluid flow in the pipe. In fact, the Navier-Stokes equations that govern this flow have been solved numerically. These equations were by an implicit method of finite differences. The systems of algebraic equations thus obtained were solved by the algorithms of Gauss and Thomas. The equation of conduction in the concrete slab was solved using the same methodology as that of flow. In this work, we based on an algorithm that interacts non stationary solid medium with a fluid medium consisting of permanent a state by ensuring equal flows and temperatures on the common interface between the two mediums at every moment. The numerical simulation of heat transfers and the thermal behavior of the heating slab were analyzed for various parameters influencing thermal diffusion. The results obtained show that the numerical methodology adopted for the control of fluid-structure coupling is acceptable in comparison with the literature.

Keywords: heated slab; thermal coupling; fluid flow; heat transfer; not stationary processes

1. INTRODUCTION

One of the renewable energy sources is solar energy, which is the most used within cities in the Mediterranean. Passive solar is a process of generating thermal energy by converting solar radiation into heat. Solar energy is the most developed compared to other renewable energies [1–3]. However, the behavior of conversion systems for this energy type is highly dependent on variations in climatic parameters such as temperature, solar irradiation and storage means [4].

In the context of thermal coupling, Giles and al. [5] have studied the numerical stability and procedures of fluid-structure thermal coupling. The aim of this study is to analysis the thermal diffusion phenomenon with a continuity of temperature and a heat quantity at the interface. Birken and al. [6] highlighted the importance of fluid-structure, thermal coupling in industrial cooling processes for the steel heat treatment [6]. This numerical study is devoted to the thermal interaction study between fluid and structure in the heating slab, also called conjugated heat transfer. Monge and Birken [7] have considered two areas with jumps in the material conductivity coefficient through the connection interface. Heuzé and al. [8]

[*] Corresponding author: abdellatif.mebarek@univ-adrar.edu.dz

have developed a digital tool to simulate the thermomechanical coupling procedure based on a fluid-structure coupling to describe the state of the structure matter throughout.

Currently, numerical simulation of fluid-structure interaction problems is one of the biggest challenges for modern scientific computing. Typical examples are found in aeronautics, where air flow around an elastic aircraft or air-sheet oscillations in air flow are well presented in the work of Dowell and al. [9]. In addition, this interaction is important in the in-Turbomachinery field, where the energy transfer will take place between a rotor and air [10]. Furthermore, in the field of biomechanics, the elastic behavior of micro-pump or artificial membranes in blood flow is affected by this type of interaction by referring to the work of Scotti and al. [11] and then Tezduyar and al. [12].

Underfloor heating is a technique that provides good comfort while minimizing energy consumption. In this context, the aim of this study is to characterize the variable heat exchange between a laminar flow of fluid in forced convection and a concrete slab of considerable thickness, the top of which is subjected to a constant ambient temperature of 28°C.

The modelling is based on the thermal balance calculation at the level for system elements: fluid-structure. Model validation was performed using the results obtained by Andreo and al [13]. The latter used the same heating system with a heat supply provided by solar energy. The second step in this work is to test the parameters influencing the heat transfer within the heating slab, analysing the system thermal behavior.

As part of this work, we propose to exploit this energy potential in the habitat through the use of a closed-circuit heating floor. Studies on floor heating technology are numerous in the North African region. We are interested in the case of a solar heating system for a single-zone space in a dry climate similar to that studied by Mokhtari and al [14]. The system is equipped with a concrete slab to store and produce heat from the floor within a habitable envelope. The principle of operation is to circulate directly into the concrete slab a fluid heated by solar collectors [15]. In fact, this slab will have the diffuser role of a soft and homogeneous heat throughout the house.

2. PHYSICAL DESCRIPTION OF THE SLAB STUDIED

The element of the numerical modelling is a hydronic heating floor which consists of three layers with a coil tube (Figure 1). The insulation material is a plate of expanded polystyrene, which is the most used in this kind of habitable constructions. The insulation layer height is 5 cm. Above it, we have a concrete screed 10 cm high, 1m long and 1m wide. In the latter are arranged the cross-linked polyethylene tubes [16,17]. They are very often used for the heated floors realization. In fact, these semi-rigid pipes are flexible, and they do not need welding to be carried out like those of copper. The tubes are arranged in (U) shape with a diameter (d) of 20 mm and a 10 cm for spacing [17]. A layer of concrete coating is superimposed on the heating grid.

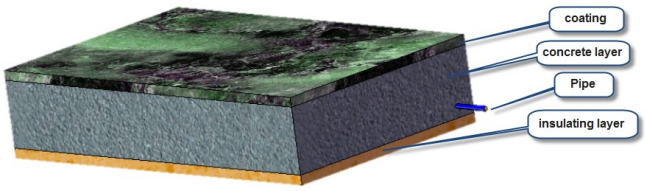

Fig.1. Physical description of the slab studied

3. MATHEMATICAL FORMULATION

3.1. Simplifying hypotheses

A set of assumptions is retained in this study to simplify the mathematical modelling for thermal transfer model. These assumptions are derived from the physical properties of fluid flow in a horizontal pipe embedded in a concrete slab.

The main assumptions taken into account in this study are as follows:

- The fluid is Newtonian, assumed to be viscous and incompressible;
- The flow is transient with a laminar regime;
- Viscous dissipation is negligible: the diffusion of purely mechanical energy is neglected because the water speed and viscosity are low;
- Flow has only two velocity components: one longitudinal speed and the other transverse;
- No internal heat sources $\varphi_S = 0$;
- The physical properties (μ, Cp, ρ, λ) are constant;
- Low pipe thickness is neglected in numerical calculations;
- The fluid-structure interface is in thermodynamic equilibrium;
- The solid medium to be isotropic.

3.2. Fluid flow modelling in the pipe

We initially opted for a flow study in a rectangular cross-section duct. This involves the flow of viscous fluid between two long plates (L), parallel and separated by a small distance (d). Both plates are fixed, and the fluid is moved by a pressure gradient (Figure 2). The solution governing a flow of Poiseuille for maximum speed (u_0) in the pipe medium is as follows [18]:

$$u_f(y) = u_0\left(1 - 4\left(\frac{y}{d}\right)^2\right) \tag{1}$$

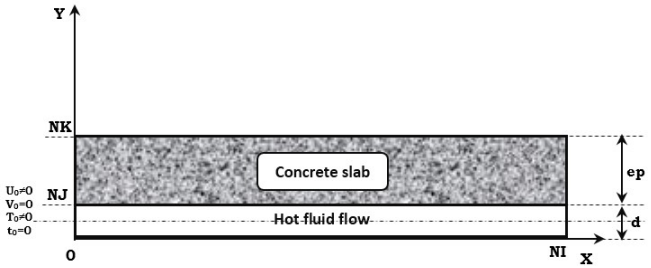

Fig.2. Physical description of fluid flow within the pipe

It should be noted that a rigorous treatment of the boundary layer would require the complete solution to Navier-Stokes equations. Their complexity prompted Prandtl to simplify them to retain only the most important terms. The main idea is to neglect the axial gradients (∂/∂x) in front of the transverse gradients (∂/∂y). Thus we obtain the Prandtl equations for boundary layer which govern a laminar flow in the heating slab pipe as follows [19,20,21]:

- *Equation the amount of movement*

$$\frac{\partial u_f}{\partial t} + u_f\frac{\partial u_f}{\partial x} + v_f\frac{\partial u_f}{\partial y} = -\frac{1}{\rho_f}\frac{\partial P_f}{\partial x} + v_f\frac{\partial^2 u_f}{\partial y^2} \quad and \quad \frac{\partial P_f}{\partial y} = 0 \tag{2}$$

- *Equation of mass conservation*

$$\frac{\partial u_f}{\partial x} + \frac{\partial v_f}{\partial y} = 0 \tag{3}$$

- *Energy conservation equation*

$$\frac{\partial T_f}{\partial t} + u_f \frac{\partial T_f}{\partial x} + v_f \frac{\partial T_f}{\partial y} = \frac{\lambda}{\rho_f \times C_{P_f}} \times \frac{\partial^2 T_f}{\partial y^2} \tag{4}$$

3.3. Mathematical model of thermal diffusion

The floor slab is regarded as a homogeneous solid to which the classical equation of heat diffusion is applied [22]. Heat diffusion is defined as a heat transmission mode in a solid caused by a temperature difference between two regions of this solid medium [23,24]. The numerical modelling is based on the two-dimensional study of heat conduction within the heating slab. The equation of thermal conduction is:

$$\frac{\partial T_b}{\partial t} = \frac{\lambda_b}{\rho_b \times C_{P_b}} \times \left(\frac{\partial^2 T_b}{\partial x^2} + \frac{\partial^2 T_b}{\partial y^2} \right) \tag{5}$$

This equation is discredited by the finite difference method using a three-point forward scheme in the contact interface. After the discretization, we get a tridiagonal algebraic system, the resolution of which is done by the Thomas algorithm.

3.4. Initial and boundary conditions

- At the moment $t = 0$, the field of calculation under consideration is initialized by:

$$u_f(0) = 0;\ v_f(0) = 0;\ T_f(0) = 0 \tag{6}$$

$$T_b(0) = 0 \tag{7}$$

- The fluid velocity at the channel inlet is given by $x = 0$ *and* $0 \le y \le d$;

$$u_f(y) = u_0 \left(1 - 4 \left(\frac{y}{d} \right)^2 \right) \tag{8}$$

- At the canal outlet we have $x = L$ *and* $0 \le y \le d$;

$$\frac{\partial u_f}{\partial x} = 0; \quad \frac{\partial v_f}{\partial x} = 0 \ \textit{and} \quad \frac{\partial T_f}{\partial x} = 0 \tag{9}$$

- The coupling interface (fluid-structure) is governed by the following expression $0 < x < L$ *and* $y = d$;

$$-\lambda_b \times \left. \frac{\partial T_b}{\partial y_b} \right|_{y_b = d} = -\lambda_f \times \left. \frac{\partial T_f}{\partial y_f} \right|_{y_f = d} \tag{10}$$

where λ_b *and* λ_f are respectively the thermal conductivities of the solid and the fluid.

- At the ambient air-slab interface we have $0 < x < L$ *and* $y = d$;

$$-\lambda_b \times \left. \frac{\partial T_b}{\partial y_b} \right|_{y_b = d} = h_c \times \left(T_b - T_{air} \right) \tag{11}$$

where *hc* convective coefficient of exchange with ambient air in ($W.m^{-2}.k^{-1}$), λ_b is the concrete thermal conductivity in ($W.m^{-1}.K^{-1}$).

- At the left edge of the slab (adiabatic walls) $x = 0$ *and* $d \le y \le d+ep$;

$$\left. \frac{\partial T_b}{\partial y} \right|_{y_b = d} = 0 \tag{12}$$

- At the right border of the slab (adiabatic walls) $x = L$ *and* $d \le y \le d+ep$;

$$\left. \frac{\partial T_b}{\partial y} \right|_{y_b = d} = 0 \tag{13}$$

- At the bottom surface of the tube (adiabatic walls) $Y = 0$ *and* $0 \le x \le L$;

$$\left.\frac{\partial T_f}{\partial y}\right|_{x_f=L} = 0 \tag{14}$$

4. COUPLING METHODOLOGY

Steady-state fluid-structure coupling has been treated many times. It involves coupling a Navier-Stokes solver to a conduction solver and searching for a stationary state in fluid and structure medium. It is to highlight that that this type of problem has already been studied digitally by Errera and al. [25]. While using the same tools, the work we present here is of a different nature. Indeed, we are interested in the non-stationary coupling and more precisely in the detailed description of the thermal exchanges in a concrete slab subjected to convective flow due to laminar flow.

4.1. Fluid-Structure Interface

Figure 3 shows the interface between two mediums with different thermal conductivities. The distance between the node (*J*) and the neighbouring nodes (*J-1 and K+1*) is calculated according to the space pitch [26,27,28].

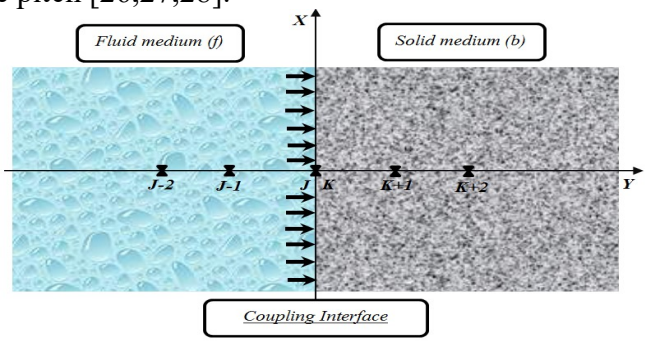

Fig. 3. Spatial discretization at the fluid-structure interface.

A finite difference formulation based on the Galerkin method was used to solve the equations that govern the fluid-structure interaction model in the heating slab [29]. In perfect contact, let us consider the case where the parietal transfer is entirely convective-conductive in nature. Regardless of the mode of convection, the transfer of energy between the surface of a solid body at temperature (T_b) and the fluid is done by thermal conduction since the fluid velocity is zero at the solid body surface. The density continuity the energy flow at the surface thus allows writing [30,31,32]:

$$\phi\big|_{(W.m^{-2})} = -\lambda_b \times \left.\frac{\partial T_b}{\partial y_b}\right|_{y_b=0} = -\lambda_f \times \left.\frac{\partial T_f}{\partial y_f}\right|_{y_f=0} \tag{15}$$

The discretization of the energy flow, density terms of the lower surface of the solid using an implicit method with finite differences to be a three-point forward scheme is given by the following expression:

$$-\lambda_b \left.\frac{\partial T_b}{\partial y_b}\right|_{y_b=0} = -\lambda_b \frac{-3.T_b(I,K)+4.T_b(I,K+1)-T_b(I,K+2)}{2.\Delta y_b} \tag{16}$$

On the other hand, the density terms discretization for energy flow at in upper surface of the fluid using of an implicit method with finite differences with a three-point back pattern is given by the following expression:

$$-\lambda_f \left.\frac{\partial T_f}{\partial y_f}\right|_{y_f=0} = -\lambda_f \frac{3.T_f(I,J)-4T_f(I,J-1)+T_f(I,J-2)}{2.\Delta y_f} \tag{17}$$

We pose:

$$C = \frac{\lambda_a}{\Delta y_a},\ \lambda_a = \frac{\lambda_b}{\lambda_f} \quad and \quad \Delta y_a = \frac{\Delta y_b}{\Delta y_f} \tag{18}$$

Or Δy_a is the relationship between the fluid spatial step and the solid spatial step, λ_a is the ratio between the solid thermal conductivity and the fluid thermal conductivity, T_f is the fluid temperature and T_b is the solid temperature.

After an equality and simplification between the two equations (16) and (17), we find the expression, of the temperature of fluid-structure coupling for the interface nodes which is given as follows:

$$T_f(I,NJ) = T_b(I,1) = \frac{C.(4.T_b(I,K+1) - T_b(I,K+2)) - (T_f(I,J-2) - 4.T_f(I,J-1))}{3.(1+C)} \tag{19}$$

5. DIMENSIONAL VARIABLES OF LOCAL EQUATIONS

To put back the equations governing the flow of the simpler fluid. A set of reduced variables (Table 1) were introduced to produce an exploitable non-dimensional form.

Table.1. Non-dimensional variables of local equations [33].

Sizes	Time	Length	Velocity	Pressure	Temperature
Ladder	t	L	u	P	T
Associated non-dimensional sizes	$t^* = \frac{u_0}{d} \times t$	$x^* = \frac{x}{d}$ et $y^* = \frac{y}{d}$	$u^* = \frac{u}{u_0}$	$P^* = \frac{2.(P-P_0)}{\rho.u_0^2}$	$T^* = \frac{T}{T_0}$
d	The pipe reference diameter				m
u_0	The maximum reference velocity at the pipe entrance				$m.s^{-1}$
$t_0 = d/u_0$	Non-dimensional reference time				s
T_0	Reference ambient temperature				°C
$\rho.u_0^2$	The reference pressure				Pa

5.1. Non-dimensional equations

In order to generalize the results, the equations governing for physical phenomenon are written in dimensionless forms based on Table 1. Non-dimensional variables are pipe diameter and input sizes (velocity and temperature). In the channel, for a two-dimensional case in cartesian coordinates, the equations system of heat and mass transfers by forced convection are formulated in the following dimensionless form [20]:

- Quantity equation of the fluid movement;

$$\frac{\partial u_f^*}{\partial t^*} + u_f^* \frac{\partial u_f^*}{\partial x^*} + v_f^* \frac{\partial u_f^*}{\partial y^*} = -\frac{\partial P_f^*}{\partial x^*} + \frac{1}{\mathrm{Re}} . \frac{\partial^2 u_f^*}{\partial y^{*2}} \tag{20}$$

- The conservation equation of fluid mass;

$$\frac{\partial u_f^*}{\partial x^*} + \frac{\partial v_f^*}{\partial y^*} = 0 \tag{21}$$

- The conservation equation of energy in the fluid;

$$\frac{\partial T_f^*}{\partial t^*} + u_f^* \frac{\partial T_f^*}{\partial x^*} + v_f^* \frac{\partial T_f^*}{\partial y^*} = \frac{1}{\mathrm{Pr}.\mathrm{Re}} . \frac{\partial^2 T_f^*}{\partial y^{*2}} \tag{22}$$

- Equation of energy conservation in the solid domain (the slab);

$$\frac{\partial T_b^*}{\partial t^*} = \frac{\lambda_b}{\rho_b \times C_{P_b} \times \nu_f} \times \frac{1}{\mathrm{Re}} \times \left(\frac{\partial^2 T_b^*}{\partial x^{*2}} + \frac{\partial^2 T_b^*}{\partial y^{*2}} \right) \tag{23}$$

$$\frac{\partial T_b^*}{\partial t^*} = \frac{\lambda_a}{(\rho.Cp)_a} . \frac{\lambda_f}{(\rho.Cp)_f} . \frac{1}{d_f . U_0} . \frac{\nu_f}{\nu_f} . \left(\frac{\partial^2 T_b^*}{\partial x^{*2}} + \frac{\partial^2 T_b^*}{\partial y^{*2}} \right)$$

$$\frac{\partial T_b^*}{\partial t^*} = \frac{\lambda_a}{(\rho.Cp)_a} . \left(\frac{\lambda_f}{(\rho.Cp)_f} . \frac{1}{\nu_f} \right) . \left(\frac{\nu_f}{d_f . U_0} \right) . \left(\frac{\partial^2 T_b^*}{\partial x^{*2}} + \frac{\partial^2 T_b^*}{\partial y^{*2}} \right) \tag{24}$$

$$\frac{\partial T_b^*}{\partial t^*} = \frac{\lambda_a}{(\rho.Cp)_a} . \frac{1}{\mathrm{Pr}} . \frac{1}{\mathrm{Re}} . \left(\frac{\partial^2 T_b^*}{\partial x^{*2}} + \frac{\partial^2 T_b^*}{\partial y^{*2}} \right)$$

Or $(\rho.Cp)_a$ is the ratio between the fluid heat capacity and that of the solid and d_f : height of the rectangular pipe.

5.2. Initial conditions and non-dimensional limits

In order to write the conditions at the boundary of two mediums in non-dimensional forms, we enter the variables in Table 1 in the equations (6 to 14) and we obtain the following expressions:

5.2.1. Non-dimensional initial conditions

- At the moment (t*), the domain of computation considered is initialized by;

$$u_f^*(0) = \frac{u_f}{u_0};\ v_f^*(0) = \frac{v_f}{u_0};\ T^*(0) = \frac{T_f}{T_0} \tag{26}$$

$$T_b^*(0) = \frac{T_b(0)}{T_0} \tag{27}$$

5.2.2. Non-dimensional boundary conditions

- The fluid velocity at the channel input is given by *x* = 0 and 0 ≤ y* ≤ 1;*

$$u_f^*(y) = u_0^* \times \left(1 - 4 \left(\frac{y^*}{1} \right)^2 \right) \tag{28}$$

- At the channel output, we have *x * = (L / d) and 0 ≤ y* ≤ 1;*

$$\frac{\partial u_f^*}{\partial x^*} = 0 \quad and \quad \frac{\partial v_f^*}{\partial x^*} = 0 \tag{29}$$

- At the fluid-structure coupling interface is governed by *0 <x*<(L / d) and y* = 0;*

$$-\lambda_a \times \left. \frac{\partial T_b^*}{\partial y_b^*} \right|_{y_b^*=1} = -\left. \frac{\partial T_f^*}{\partial y_f^*} \right|_{y_f^*=1} \tag{30}$$

- At the top surface of the slab [27], we have *0 <x* < (L/d) and y* = 1 + (ep/d);*

$$-\lambda_a \times \left. \frac{\partial T_b^*}{\partial y_b^*} \right|_{y_b^*=1+(ep/d)} = 1 \times \left(T_b^* - T_{air}^* \right) \tag{31}$$

With:

($h^*_c=h_c/h_0$) is the convective exchange coefficient with the ambient air.

- At the slab left border (adiabatic walls) $x^* = 0$ *and* $1 \leq y \leq 1+(ep/d)$;

$$\left.\frac{\partial T_b^*}{\partial y^*}\right|_{y_b^*=d} = 0 \tag{32}$$

- At the slab right boundary (adiabatic walls) $x^* = L$ *and* $1 \leq y \leq 1+ (ep/d)$;

$$\left.\frac{\partial T_b^*}{\partial y^*}\right|_{y_b^*=d} = 0 \tag{33}$$

- At the tube bottom surface (adiabatic walls) $Y^* = 0$ *and* $0 \leq x^* \leq L/d$;

$$\left.\frac{\partial T_f^*}{\partial x^*}\right|_{x_f^*=L} = 0 \tag{34}$$

6. FLOW CHART OF FLUID-STRUCTURE THERMAL COUPLING

The flowchart in Figure 4 shows the procedure for calculating the temperature at the slab top surface by following the following steps:

- Requisitions of the physico-thermal properties for fluid-structure system;
- Initialization of the system at room temperature (28 °C);
- Resolution of Navier-Stokes equations in the field of fluid;
- Solving the of the conduction equation in the slab;
- Coupling temperature test;
- Test on the calculation overall time;
- Recording the results obtained.

7. DATA FROM THE NUMERICAL SIMULATION

Table 2 shows the physico-thermal properties of air, concrete and water, which are used in numerical simulation.

Table.2. Physico-thermal properties of the studied domain [14,13,34,35].

Physico-thermal properties		Air	$Water_{(ref)}$	Concrete
Cp	Specific heat in ($J.Kg^{-1}.K^{-1}$)	1006	4182	880
ρ	Density in ($Kg.m^{-3}$)	1,177	1000	2000
μ	Dynamic viscosity in ($Kg.m^{-1}.s^{-1}$)	$1,85.10^{-5}$	10^{-3}	-
υ	Kinematic viscosity in ($m^2.s^{-1}$)	$1,75.10^{-5}$	10^{-6}	-
λ	Thermal conductivity in ($W.m^{-1}.K^{-1}$)	0,0262	0,597	1,75
Pr	Number of Prandtl	0,708	7,01	-

The constants used for numerical resolution of the problem studied are [13];

- Heat exchange coefficient: $h_c=8,12\ W.m^{-2}.k^{-1}$;
- Ambient air temperature: $T_{air}=28°C$;
- Fluid inlet temperature: $T_e = 60\ °\ C$;
- Reynolds number: $Re = 500$;
- Step time of time: $\Delta t = 10s$.

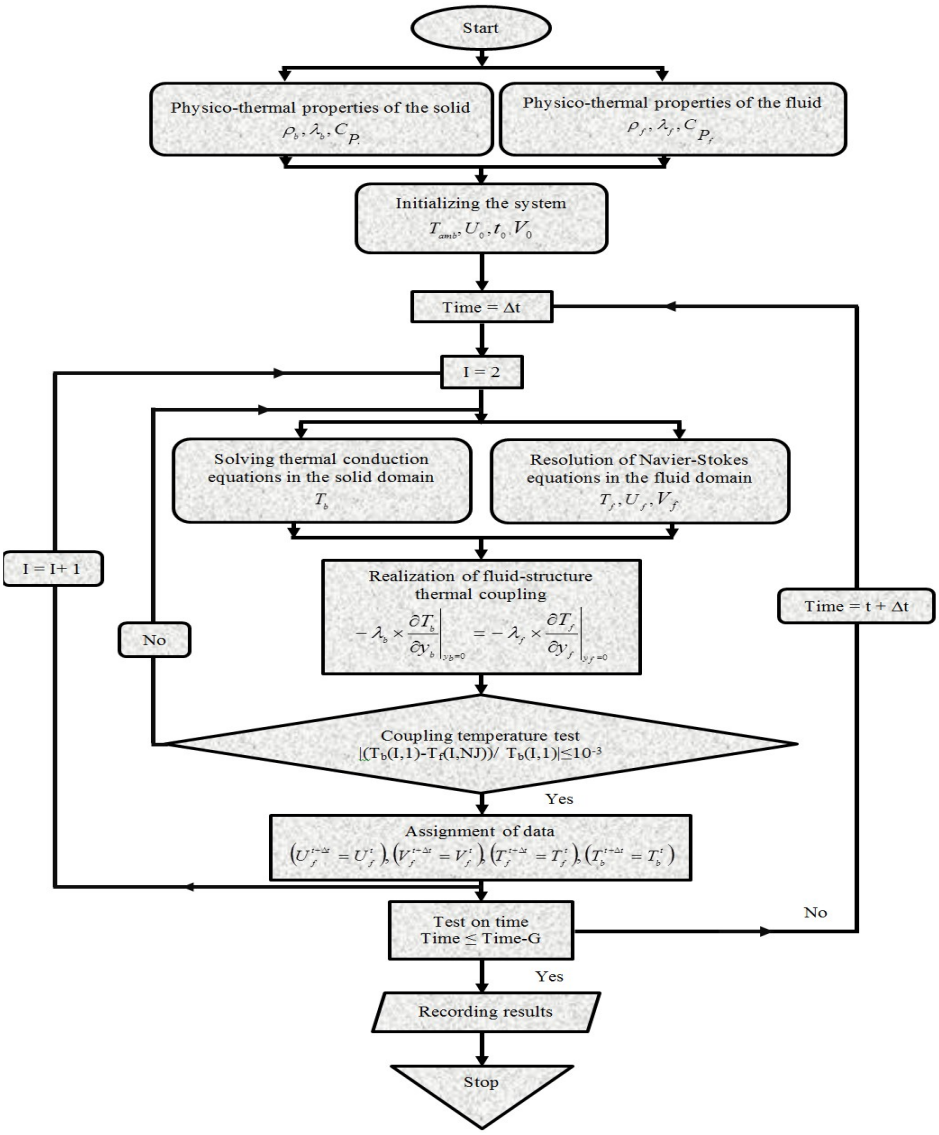

Fig.4. Flowchart of the numerical modeling of fluid-structure thermal coupling.

The data of the calculation grid in the two fluid-structure subdomains are presented in Table 3:

Table. 3. Calculation grid data in the fluid-structure domain.

	Length (m)	Height (mm)	*NI*	*J*	*NK*	Δ*X*	Δ*Y*	Time step Δt (s)
Fluid	1	20	101	41	-	10^{-2}	$5x10^{-4}$	10
Structure		10	101	-	81		$1,25x10^{-3}$	
NI	Node indices on the x-axis of the two calculation domains.							
NJ	Node indices on the y-axis of the fluid domain.							
NK	Node indices on the y-axis of the solid domain.							
Δ*X*	Step space on the x-axis of the two calculation domains.							
Δ*Y*	Step space on the y-axis of the two calculation domains.							
Δ*t*	Calculation increment time.							

8. RESULTS AND DISCUSSIONS

8.1. Validation of the numerical model

Figure 5 shows the temperature evolution of a point on the slab upper surface as a function of time. It is noted that there is an acceptable agreement between the results obtained by the developed model and those of Andreo and al [13], so Mokhtari and al [14] with relative errors equal to 5,04% and 1,77% respectively.

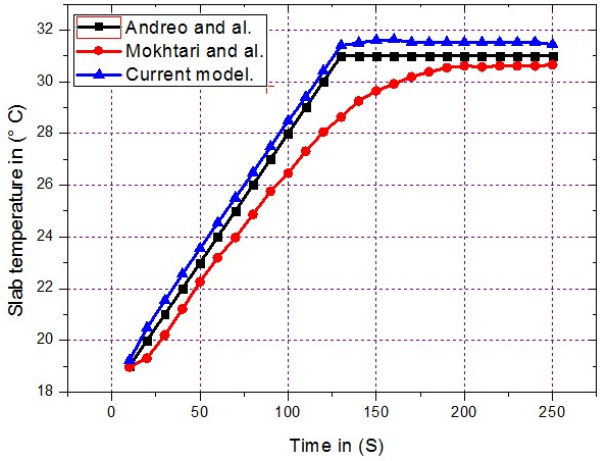

Fig.5. Evolution of the temperature profile at a point in the slab medium as a function of the overall time.

8.2. Evolution of the concrete slab temperature according to the spacing step

Figure 6 shows the variation in the heating slab temperature as a function of the space pitch ratio for four times. This variation has been highlighted for three different positions in the system (at the inlet, the medium and at the outlet). We can notice that:

- The evolution of thermal diffusion in the concrete slab is almost similar for the three positions considered (inlet, medium and outlet);
- There is a remarkable temperature difference between the positions in the system for the four selected global calculation times;
- For a ratio of space varying between 0 and 0.12 with a fluid inlet temperature in the pipe at 60°C, the heat propagation in the solid decreases almost to temperature values (in the medium) of about 38°C for t = 3600s (Fig. 6.a), 47°C for t = 10800s (Fig. 6.b), 48°C for t = 14400s (Fig. 6.c) and 49°C for t = 43200s (Fig. 6.d).

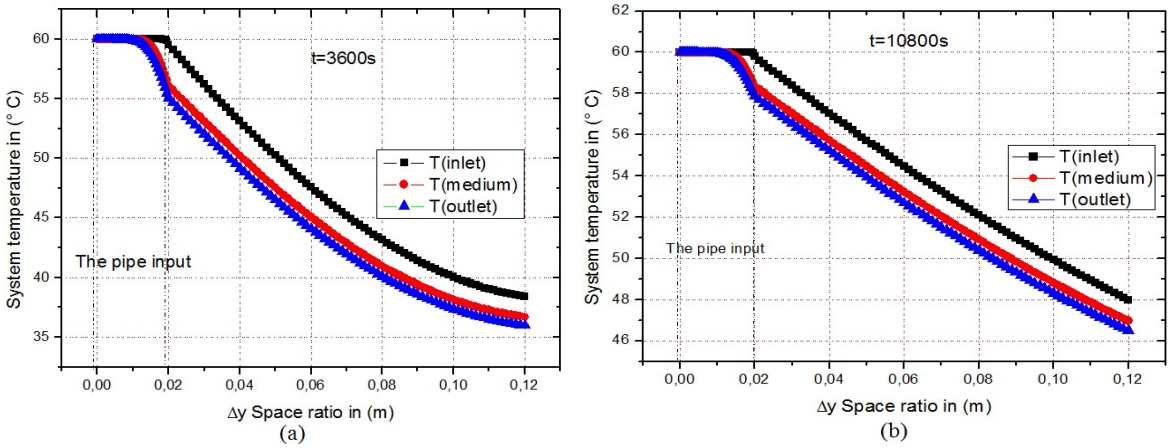

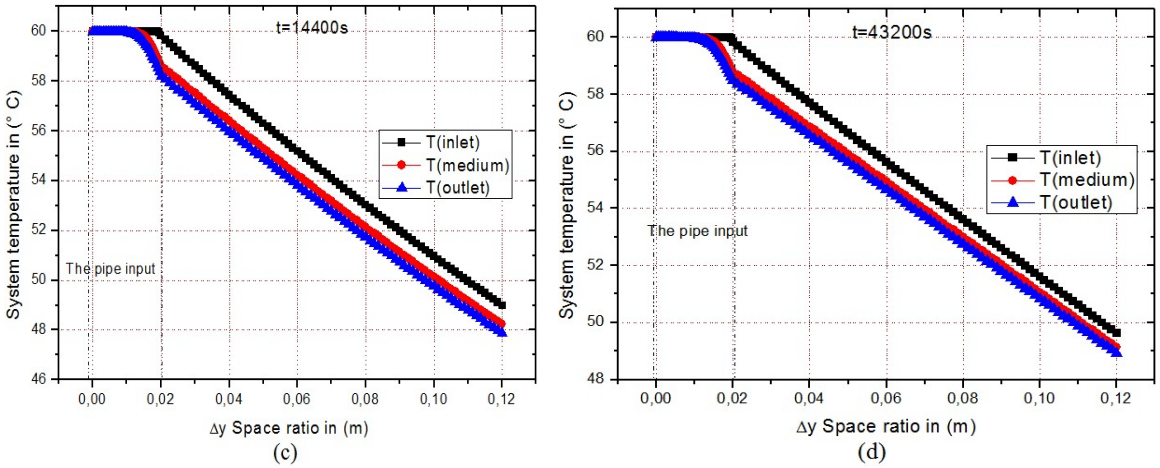

Fig.6. Comparison between the three profiles (input, medium and output) of the temperature as a function of the slab space pitch ratio for (a) t = 3600s, (b) t = 10800s, (c) t = 14400s and (d) t = 43200s

8.3. Evolution of the system temperature for different thicknesses of the slab

Figure 7 illustrates the change in temperature in the medium slab as a function of time for different thicknesses of the concrete top layer. It is clear that the heat propagation in the slab decreases considerably with the increase in the thickness of the upper layer the concrete. That is to say, when the concrete thickness is decreased (for example 10 cm), the evolution of the temperature increases rapidly as a function of time and vice versa. In other words, the heat diffusion in the room will be even lower than the concrete mass is important.

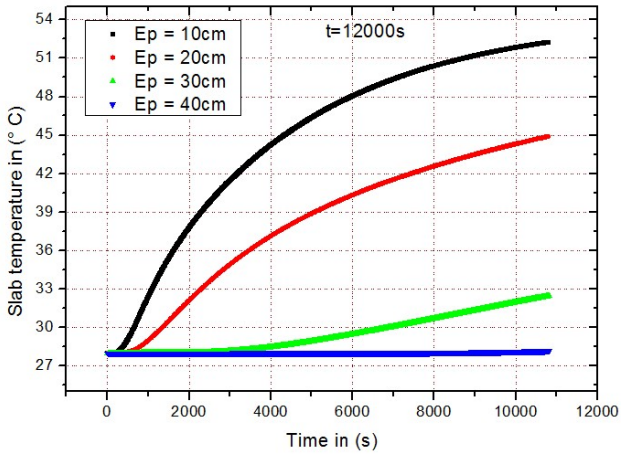

Fig.7. Evolution of the temperature profile in the slab as a function of time for different thicknesses of the concrete

8.4. Effect of variation of the convective exchange coefficient with the ambient air

Figure 8 shows the evolution of heating slab temperature as a function of time for different convective coefficients with ambient air. It can be observed that when the value of the convective exchange coefficient increases, the thermal diffusion increases slightly and vice versa. It should also be noted that the variation for convective exchange coefficient with ambient air has a notable influence on the thermal diffusion of heat within the heating slab. In addition, we will note that the evolution of the temperature will start from 28°C, the atmosphere temperature , and it will increase over time to the highest value around 60°C, which is the temperature at which the fluid inlet the slab pipe.

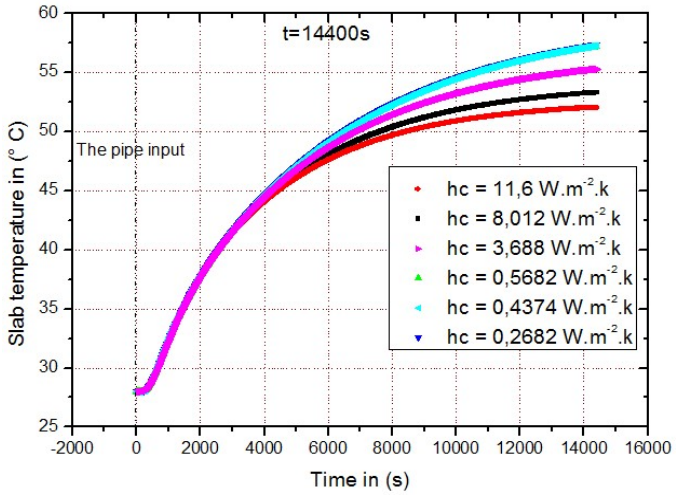

Fig.8. Evolution of the heating slab temperature as a function of time for different convective coefficients with ambient air

8.5. Evolution of the velocity profile of the fluid in the pipeline

The evolution of fluid velocity within the pipe as a function of the space step for different Reynolds numbers is illustrated in Figure 9. In this figure, it can be seen that the shape of the fluid velocity profile in the pipe is parabolic. In addition, it keeps the same shape, but its maximum value increases with the increase in the number of Reynolds or it reaches a maximum value equal to 0,0175m/s for Re = 800. This evolution shows that the variation influence of the Reynolds number on the fluid flow is important.

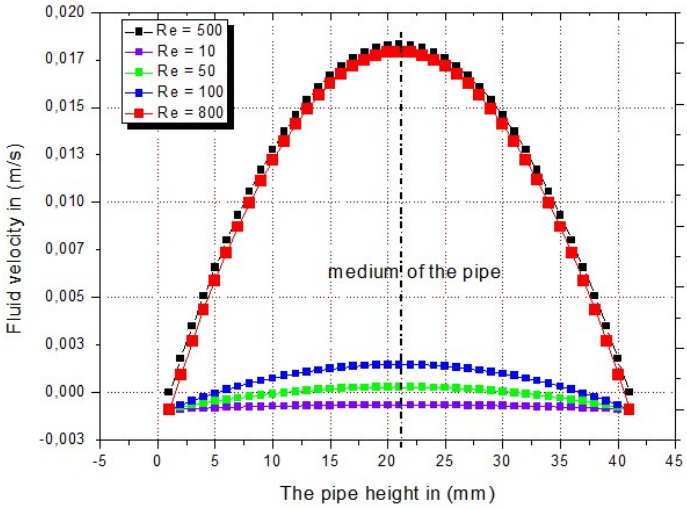

Fig. 9. Profiles of fluid velocities within the pipe versus space step for different Reynolds numbers

9. CONCLUSION

The objective of this digital study is the adaptation of a numerical methodology in order to be able to control and characterize the thermal exchanges within a heating slab intended for heating by the ground. In fact, we analyzed the temperature evolution at the inlet, medium and outlet of the system according to the space step. In addition, we analyzed the evolution of the slab temperature for different thicknesses of the concrete and also the effect of variation of the convective exchange coefficient with the ambient air on the surface temperature of the slab. On the other hand, we have highlighted the effect of the Reynolds number variation on the evolution of the fluid velocity profile in the pipe.

The validity of this numerical approach is confirmed based on the work done by Mokhtari and Andreo. The methodology we have presented makes it possible to analyses the thermal

transient phase over very short periods of time using the current numerical model of fluid-structure thermal coupling.

Nomenclature

Cp	Heat capacity.	$W.m^{-1}.K^{-1}$
d	Pipe diameter.	m
Ep	Concrete thickness.	m
hc	Convective coefficient with ambient air.	$W.m^{-2}.K^{-1}$
h_0	Convective coefficient reference.	$W.m^{-2}.K^{-1}$
I	Index of the abscissa axis incrementation.	-
L	Pipe length.	m
J	Index of the ordinate axis incrementation in the fluid domain.	-
k	Increment index of the y-axis in the solid domain.	-
Pr	Number of Prandtl.	-
P_f	Fluid pressure.	Pas
φ_s	The internal heat quantity.	$W.m^{-2}$
Re	Number of Reynolds.	-
T_{air}	Air temperature.	K
T_e	Inlet temperature of the fluid in the pipe.	K
T_{milieu}	Temperature in the slab middle.	K
$T_{entrée}$	Temperature at the pipe entrance.	K
T_{sortie}	Temperature at the pipe outlet.	K
T^*	Dimensional temperature.	-
T_f	Fluid temperature.	K
T_b	Concrete temperature.	K
t	Time.	s
U_0	Initial longitudinal velocity of the fluid.	$m.s^{-1}$
U^*	Dimensional longitudinal velocity of the fluid.	-
V_f	Initial transverse velocity of the fluid.	$m.s^{-1}$
V^*	Initial transverse velocity of the fluid.	-
y	Directional normal of the fluid diffusivity.	-
Greek symbols		
λ	Thermal conductivity.	$W.m^{-1}.K^{-1}$
λ_a	Report between of the fluid thermal conductivity and the solid.	-
μ	Dynamic viscosity of the fluid.	$Kg.m^{-1}.S^{-1}$
ρ	Volumic mass.	$Kg.m^{-3}$

REFERENCES

[1] Mehdary A., Naamane A., M'sirdi K. (2011), ‘’Real Time Implementation Control for multi-source energy system’’, *Sustainability in Energy and Building*, Page 524.

[2] Ky Le. (2008),’’ Gestion optimale des consommations d'énergie dans les bâtiments’’. *Thesis P.h.D*, soutenu le 10 Juillet 2008. Laboratoire de génie électrique, Institut Polytechnique de Grenoble, la France.

[3] Tina G. and Scrofani S. (2008), ‘’ Electrical and thermal model for PV module temperature evaluation’’. *IEEE Electro technical Conference*, Pages 585-590.

[4] Abarkan M. (2014), ‘’Modélisation et Analyse du comportement d'un Bâtiment équipé d'un Système Multi Sources d'énergie’’, *Thesis P.h.D* de l’Université Aix-Marseille, la France.

[5] Giles M. B. (1997), ''Stability analysis of numerical interface conditions in fluid-structure thermal analysis'', *International journal for numerical methods in fluids*, vol. 25, 421-436.

[6] Birken P., Quint K., Hartmann S. and Meister A. (2010), A time-adaptive fluid-structure interaction method for thermal coupling'', *Comput Visual Sci.(2010) 13:331–340*, DOI 10.1007/s00791-010-0150-4.

[7] Monge A. and Birken P. (2018), ''On the convergence rate of the Dirichlet–Neumann iteration for unsteady thermal fluid–structure interaction'', *Comput Mech (2018) 62-525*, doi.org/10.1007/s00466-017-1511-3.

[8] Heuzé T., Leblond J. B. and. Bergheau J. M. (2011), ''Modélisation des couplages fluide/solide dans les procédés d'assemblage à haute température'', *Mécanique & Industries* (12), 183–191.

[9] Dowell E., Thomas J. and Hall K. (2004), ''Transonic limit cycle oscillation analysis using reduced order aerodynamic models'', *Journal of Fluids and Structures* (19), 17–27.

[10] Willcox K., Paduano J. and Peraire J. (1999), ''Low order aerodynamic models for aeroelastic control of turbomachines''. *In 40th AIAA ASME ASCE AHS ASC structures*, structural dynamics and materials conference, St Louis, MO.

[11] Scotti C. and Finol E. (2007), ''Compliant biomechanics of abdominal aortic aneurysms: a fluid–structure interaction study'', *Computers and Structures*, (85), 1097–1130.

[12] Tezduyar T. E., Schwaab M. and Sathe S. (2008), ''Sequentially-coupled arterial fluid-structure interaction (scafsi) technique'', *Computer Methods in Applied Mechanics and Engineering*.

[13] Ugo A., Fabien B. and Adeline V. (2015), ''Etude de la diffusion de la chaleur dans un plancher chauffant en environnement terrestre'', *étude de l'université de Paul Sabatier*, Toulouse III, la France.

[14] Mokhtari F., Ait Messaoudène N., Hamid A. and Belhamel M. (2006), ''Etude du comportement thermique d'une maison munie d'un système de chauffage solaire'', *Revue des Energies Renouvelables* Vol. 9 N°4, 363 – 370.

[15] Sobhy I., Brakez A. and Benhamou B. (2014), ''Modélisation dynamique du comportement thermique d'un plancher chauffant avec circuit fermé à Marrakech'', *1ere Colloque Franco-Marocain sur les Energies Renouvelables*, COFMER'01, Rabat 28-30.

[16] Fiche Technique Tube PER Prégainé (2016), 91, Rue Duruisseau, PA des Chesnes – 38297 St Quentin – Fallavier, Date de mise à jour : 22/06/16.

[17] Oudrane A., Aour B. and Benhamou M. (2016), ''Étude et analyse paramétrique d'une installation solaire : plancher solaire dicte d'implanter dans la région d'Adrar'', *ElWahat pour les Recherches et les Etudes* Vol.9 n°1, 27 – 49.

[18] Noel E. and Delaune M. (2012), ''Simulation numérique des équations de Navier-Stokes'', *Projet de Physique P6-3 STPI/P6-3/2011–39*, institut national des sciences appliquées de Rouen département sciences et techniques pour l'Ingénieur, de l'université -76801 Saint Etienne du Rouvray.

[19] Marty P. (2012), ''Transferts thermiques convectifs'', Génie des Procédés Master 2, Université Joseph Fourier, Grenoble, version modifiée.

[20] Hassine N. B., Chesneau X. and Laatar A. H. (2017), ''Numerical simulation of heat and mass transfers during solar drying of sewage sludge: Radiation effect'', *Energy Procedia* (139), 804–809.

[21] Abdul Aziz M. S. and Abdullah M. Z. (2014), ''Thermal Fluid-Structure Interaction in the Effects of Pin-Through-Hole Diameter during Wave Soldering'', *Hindawi Publishing Corporation Advances in Mechanical Engineering* Volume 2014,Article ID 275735, 13 pages, doi.org/10.1155/2014/275735.

[22] Oudrane A., Aour B., Hamouda M. and Benhamou M. (2016), ''Méthodologie pour la détermination de l'écartement optimal de la chaîne tubulaire d'une dalle chauffante'', *Revue des Energies Renouvelables* Vol. 19 N°1, 11 – 19.

[23] Debard Y. (2011), ''Méthode des ´éléments finis : thermique, Master Modélisation Numérique et Réalité Virtuelle'', Université du Mans, la France.

[24] Chiasson A. D., Spitler J. D. and Rees S. J. (2000), ''A Model for simulating the performance of a pavement heating system as a supplemental heat rejecter with closed-loop ground-source heat pump systems'', *Journal of Solar Energy Engineering*, Vol. 122,183-191.

[25] Errera M. P., Chaineray G. and Chemin S. (2007), ''Etude du transitoire thermique dans un matériau via un couplage convection-conduction'', *Congrès Français de Thermique*, SFT 2007, Île des Embiez, 29 mai - 1 juin 2007.

[26] Saatdjian E. (1998), ''Phénomènes de transport et leurs résolutions numériques'', *2éme édition, Polytechnica*, 15 rue Lacépède F-75005, ISBN2-84045-057-6, Paris, la France.

[27] Florides G. and Kalogirou S. (2007), ''Ground heat exchangers—A review of systems: models and applications'', *Renewable Energy* (32), 2461–2478.

[28] Ghalambaz M., Jamesahar E., Ismael A. and Chamkha J. (2017), ''Fluid-structure interaction study of natural convection heat transfer over a flexible oscillating fin in a square cavity'', *International Journal of Thermal Sciences* (111), 256-273.

[29] Al-Amiri A. and Khanafer K. (2011), ''Fluid–structure interaction analysis of mixed convection heat transfer in a lid-driven cavity with a flexible bottom wall'', *International Journal of Heat and Mass Transfer* 54, pp.3826–3836.

[30] Mergui S. (2010), ''Transferts thermiques'', *licence de mécanique 2éme année*, UPMC, université de Sorbonne.

[31] Abide S., Viazzo S. and Solliec C. (2018), ''Simulation numérique du refroidissement d'une plaque plane par un jet plan impactant'', *LAMPS-GME, Université de Perpignan*, 52 Avenue Paul Alduy, 66860 Perpignan, la France. https://docplayer.fr/25679830-Simulation-numerique-du-refroidissement-d-une-plaque-plane-par-un-jet-plan impactant.html, (Page consulté le 29/05/2018).

[32] Gobin D., Levesque D. and Benard C. (1979), ''Stockage de l'énergie solaire : simulation numérique du transfert d'énergie par conduction et rayonnement dans un milieu à deux phases'', *revue de physique appliquée*, tome 14, page 125.

[33] Mahdaoui H., Chesneau X. and Laatar A. H. (2017), ''Numerical simulation of flow through a porous cylinder'', Energy Procedia (139), 785-790.

[34] Chahwane L. (2011), ''Valorisation de l'inertie thermique pour la performance énergétique des bâtiments'', *P.h.D Thesis* de l'université de Grenoble, la France.

[35] Oudrane A. (2018), ''Contribution à la modélisation et au développement des systèmes de chauffage solaire à usage individuel'', *P.h.D Thesis* d'Ecole Nationale Polytechnique d'Oran - Maurice Audin, Algérie.

